# Optimal FPE for non-linear 1d-SDE. I: Additive Gaussian colored noise

Journal of Physics Communications

OPEN ACCESS

RECEIVED
14 July 2020

REVISED
30 September 2020

ACCEPTED FOR PUBLICATION
28 October 2020

PUBLISHED
12 November 2020



PAPER

# Optimal FPE for non-linear 1d-SDE. I: Additive Gaussian colored noise

**Marco Bianucci**[1] **and Riccardo Mannella**[2]

[1] Istituto di Scienze Marine, Consiglio Nazionale delle Ricerche (ISMAR—CNR), Forte Santa Teresa, Pozzuolo di Lerici, 19032 Lerici (SP), Italy

[2] Dipartimento di Fisica, Università di Pisa, 56100 Pisa, Italy

**E-mail:** marco.bianucci@cnr.it

**Keywords:** Fokker Planck equation, non linear stochastic processes, non linear diffusion equation

## Abstract

Many complex phenomena occurring in physics, chemistry, biology, finance, etc can be reduced, by some projection process, to a 1-d stochastic Differential equation (SDE) for the variable of interest. Typically, this SDE is both non-linear and non-Markovian, so a Fokker Planck equation (FPE), for the probability density function (PDF), is generally not obtainable. However, a FPE is desirable because it is the main tool to obtain relevant analytical statistical information such as stationary PDF and First Passage Time. This problem has been addressed by many authors in the past, but due to an incorrect use of the interaction picture (the standard tool to obtain a reduced FPE) previous theoretical results were incorrect, as confirmed by direct numerical simulation of the SDE. The pitfall lies in the rapid diverging behavior of the backward evolution of the trajectories for strong dissipative flows. We will show, in general, how to address this problem and we will derive the correct best FPE from a cumulant-perturbation approach. The specific perturbation method followed gives general validity to the results obtained, beyond the simple case of exponentially correlated Gaussian driving used here as an example: it can be applied even to non Gaussian drivings with a generic time correlation.

## 1. Introduction

In the present work we are interested in non-linear 1-d SDEs of the form:

$$\dot{X} = -C(X) + \epsilon\xi(t). \tag{1}$$

where $X$ is the variable of interest, $-C(X)$ is the unperturbed drift field, $\xi(t)$ is the stochastic Gaussian perturbation with zero mean and autocorrelation function $\varphi(t,\, t') = \langle \xi(t)\xi(t')\rangle / \langle \xi^2 \rangle$, the parameter $\epsilon$ controls the intensity of the perturbation, and $\langle ... \rangle$ implies average over the $\xi$ realizations. The SDE in (1) is ubiquitous in many research fields [1].

We consider here a simple additive and Gaussian SDE because we want to focus on a flaw that plagued previous applications of the perturbation method to dissipative systems, and which is solved here. However, the extension of the present approach to the case of multiplicative correlated noise, possibly non-Gaussian, is straightforward, although it presents some subtleties, and it will be dealt with in a later work.

It is a standard result in statistical physics that when the stochastic forcing $\xi$ is a 'white noise', $\langle \xi(t)\xi(t')\rangle = 2\,\delta(t - t')$, (1) leads to a flow for the Probability Density Function (PDF) $P(X; t)$ of the variable $X$ equivalent to the probability flow given by the following Fokker Planck equation (FPE) (where $\partial_X := \partial/\partial X, D_0 = \epsilon^2$.):

$$\partial_t P(X;\, t) = \partial_X C(X) P(X;\, t) + D_0\, \partial_X^2 P(X;\, t). \tag{2}$$

From (2), the stationary PDF is given by

$$P_{W,eq}(X) = \frac{1}{Z} e^{-\int^X \frac{C(y)}{D_0}\, dy} \tag{3}$$

where $Z$ is a normalization constant.

However, white noise is often an oversimplification of the real driving acting on a system of interest. Correlated noise (termed 'colored' in the literature) is more common in continuous systems, and its importance has been recognized in a large number of very different situations, like for instance statistical properties of dye lasers [2–5] and laser technology [6], chemical reaction rate [7–10], optical bistability [11, 12], stochastic resonance [13] large scale Ocean/Atmosphere dynamics [14, 15], nonlinear energy harvesting systems [16], sensors design [17], ecosystems [18–20], medical sciences [21–23], neural systems [24, 25], material science [26, 27] and many others.

We will assume that the stochastic process $\xi(t)$ is characterized by a 'finite' correlation time $\tau$[3] and unitary intensity $\langle\xi^2\rangle\tau = 1$. It is well known that if the unperturbed drift field is linear, regardless of the number of dimensions, the Gaussian property of a generic colored noise $\xi(t)$ is 'linearly' transferred to the system of interest, so the FPE structure does not break (see, e.g., [10, 28]). On the contrary, in the case of non linear SDE and/or non Gaussian noise, for finite values of $\tau$ the FPE structure breaks down. This is the case of interest here, and the aim of this paper is to recover in some appropriate limits a FPE structure, obtaining an effective FPE with a state dependent diffusion coefficient:

$$\partial_t P(X;\, t) = \partial_X C(X) P(X;\, t) + \partial^2_{X^2} D(X) P(X;\, t) \tag{4}$$

that, with a good approximation, could describe the evolution and the stationary properties of $P(X; t)$. Given $D(X)$, the stationary PDF of the FPE of (4) is then easily obtained

$$P_s(X) = \frac{1}{Z}\frac{e^{-\int^X \frac{C(Y)}{D(Y)}dY}}{D(X)} \tag{5}$$

Several techniques have been developed to deal with the correlation time of the noise in nonlinear SDE, with the aim of eventually obtaining this effective FPE. They can be grouped in three main categories that correspond to three general techniques: the cumulant expansion technique [29–31], the functional-calculus approach [21, 32–38] and the projection-perturbation methods (e.g., [9, 39–41]). Each of these methods leads to a formally exact evolution equation for the PDF of the driven process, and the different descriptions are therefore equivalent. The exact formal results do not lend themselves to calculations nor give a FPE structure, therefore they require that approximations be made. The approximations made within these various formalisms involve truncations and/or partial resummations of infinite power series with respect to $\epsilon$ and $\tau$, which are typically the small parameters in the problem. Not surprisingly, it has been argued [38] that the effective FPE obtained from the different techniques are identical, if the same approximations are made (time scale separation, weak perturbation, Gaussian noise etc.). The results of the approximations can be grouped in three categories: the 'Best Fokker Plank equation' (BFPE) obtained by Lopez, West and Lindenberg [38] from a standard perturbation method, where $\epsilon$ is the small parameter and $\tau$ is finite but (in general) not limited, the 'Local Linearization Assumption' (LLA) FPE, that formally can be considered as a small $\tau$ expansion of the BFPE (see section 4), and that has been obtained in different ways, e.g., by Grigolini [42], exploiting an ad-hoc projection procedure, or by Fox [33, 34], Hänggi [35–37] and the Barcelona group [43–46], using functional-calculus, and, finally, the gen-FPE, that makes use of moments of the unknown response PDF [21, 32] and that, improving the old cited functional-calculus approach, leads to anon linear FPE for values of $\epsilon^2\tau$ enough large to include all cases of interest. It is also worth mentioning the Unified Colored Noise Approximation (UCNA) [47, 48], a filtering approach introduced by Yung and Hänggi for a general stochastic dynamic systems driven by a Gaussian *red noise* (a Ornstein-Uhlenbeck process). The UCNA approach is based on two steps: taking advantage of the simple characteristics of red noise, the number of degrees of freedom is increased, so to obtain a multidimensional *white noise* SDE. Then, under the condition of small or large correlation times $\tau$, the number of degrees of freedom is reduced back to the original one, holding the white nature of the noise. In the limit of small $\tau$ the equivalent FPE coincides, of course, with the LLA one, but for large $\tau$ it is different. However, it is notable that the *stationary* PDF of the UCNA FPE always coincides with that of the LLA FPE [36, chap.IV]. Apart from the limitations, already highlighted, of the UCNA method, filtering approaches have the inherent drawback of increasing the degrees of freedom in the FPE equation when an accurate approximation is needed. A separate consideration deserves some interesting recent works on the gen-FPE [49, 50]. The approximation scheme is based on an extension of the Novikov–Furutsu theorem and on a stochastic Volterra–Taylor functional expansion around the instantaneous values of appropriate response moments [50]. The results are not limited to the red noise case and are in excellent agreement with numerical simulations of the SDE in both the transient and long-time regimes, for any correlation function of the stochastic perturbation (assuming the

[3] The general prescription is that there is a time $\tau$ such that, for any time $t$, the instances of $\xi$ at times $t' > t + \tau$ are 'almost statistically uncorrelated' with the instances of $\xi$ at times $t' < t$. For 'almost statistically uncorrelated' we mean that the joint probability density functions factorizes up to terms $O(\tau)$: $p_n(\xi_1, t_1'; \xi_2, t_2'; ...; \xi_k, t_k'; \xi_{k+1}, t_1; ...; \xi_n, t_h) = p_k(\xi_1, t_1'; \xi_2, t_2'; ...; \xi_k, t_k') p_h(\xi_{k+1}, t_1; ...; \xi_n, t_h) + O(\tau)$ with $k, h, n \in \mathbb{N}, k + h = n$ and $t_i' > t_j + \tau$. For example, $p_2(\xi_1, t'; \xi_2, t) = p_1(\xi_1, t') p_1(\xi_2, t) + O(\tau)$.

system is stable). But, they are intrinsically limited to the case of 1-d correlated Gaussian noise and the gen-FPE has a nonlinear/non-local structure. Although this latter fact does not pose many difficulties in the numerical simulations (the nonlinearity and the non-locality appear in the diffusion coefficient(s)), it does not allow to directly use standard simple analytical tools developed for linear FPE as the eigenvalues approach or the Mean First Passage techniques (see, e.g., [51, Chap. 5]).

In this work we focus our attention to the linear FPE to be associated, with good approximation, to SDE with general correlated Gaussian noise. Moreover we want to use an approach that leaves open the possibility of including non Gaussian perturbations. Thus, the BFPE looks as the perfect candidate.

Although, as mentioned, the LLA FPE can be formally considered a small $\tau$ expansion, strangely enough, the BFPE often fails when compared with numerical simulations, even for relatively weak perturbations, while the LLA FPE usually works better.

In section 2 we will shortly review the perturbation approach that leads to the BFPE, stressing that care must be taken when using the interaction picture in strongly dissipative systems: the pitfalls we will point out are the sources of the problems with the original formulation of the BFPE. Section 3 is the main section of the present work: we will show how to cure the shortcomings of the BFPE pointed out in section 2. Section 4 is devoted to a comparison with the LLA results. In section 5 we present the conclusions.

## 2. The standard BFPE

From (1) it follows that, for any realization of the process $\xi(u)$, with $0 \leqslant u \leqslant t$, the time-evolution of the PDF of the whole system, which we indicate with $P_\xi(X; t)$, satisfies the following PDE:

$$\partial_t P_\xi(X;\, t) = \mathcal{L}_a\, P_\xi(X;\, t) + \epsilon\ \xi(t)\mathcal{L}_I\, P_\xi(X;\, t) \tag{6}$$

in which the unperturbed Liouville operator $\mathcal{L}_a$ is

$$\mathcal{L}_a \coloneqq \partial_X C(X) \tag{7}$$

and the Liouville perturbation operator is

$$\mathcal{L}_I \coloneqq \partial_X. \tag{8}$$

A standard step of the perturbation method is to introduce the interaction representation, by which (6) becomes

$$\partial_t \tilde{P}_\xi(X;\, t) = \epsilon\xi(t)\tilde{\mathcal{L}}_I(t)\tilde{P}_\xi(X;\, t), \tag{9}$$

where

$$\tilde{P}_\xi(X;\, t) \coloneqq e^{-\mathcal{L}_a t} P_\xi(X;\, t), \tag{10}$$

and

$$\tilde{\mathcal{L}}_I(t) \coloneqq e^{-\mathcal{L}_a t}\mathcal{L}_I e^{\mathcal{L}_a t} = e^{-\mathcal{L}_a^\times t}[\mathcal{L}_I], \tag{11}$$

where, for any couple of operators $\mathcal{A}$ and $\mathcal{B}$, we have defined $\mathcal{A}^\times[\mathcal{B}] \coloneqq [\mathcal{A},\, \mathcal{B}] = \mathcal{A}\mathcal{B} - \mathcal{B}\mathcal{A}$. The last step in (11) is easily proved by induction and it is known as the Hadamard's lemma for exponentials of operators. In [31] $\tilde{\mathcal{L}}_I(t)$ of (11) is also called the Lie evolution of the operator $\mathcal{L}_I$ along the Liouvillian $\mathcal{L}_a$, for a time $-t$. For further use, we note that the Lie evolution of a product of operators is the product of the Lie evolution of the individual operators:

$$e^{\mathcal{A}^\times t}[\mathcal{B}\mathcal{C}] = e^{\mathcal{A}^\times t}[\mathcal{B}]\ e^{\mathcal{A}^\times t}[\mathcal{C}]. \tag{12}$$

Integrating (9) and averaging over the realization of $\xi(t)$, we get

$$\tilde{P}(X;\, t) = \left\langle \overleftarrow{\exp}\left[\epsilon \int_0^t du\ \xi(u)\tilde{\mathcal{L}}_I(u)\right]\right\rangle P(X;\, 0) \tag{13}$$

where $\overleftarrow{\exp}[...]$ is the standard chronological ordered exponential (from right to left), $P(X;\, t) \coloneqq \langle P_\xi(X;\, t)\rangle$ and we assumed that $P_\xi(X; 0) = P(X; 0)$, i.e. at the initial time $t = 0$ $P_\xi(X; 0)$ does not depend on the possible values of the process $\xi$, or that we wait long enough to make the initial conditions irrelevant. The result of (13) is exact, no approximations have been introduced at this level.

The r.h.s. of (9) can be considered as a sort of generalized moment generating function for the fluctuating operator $\xi(u)\tilde{\mathcal{L}}_I$ to which it is possible to associate a generalized cumulant generating function [52]:

$$\left\langle \overleftarrow{\exp}\left[\epsilon \int_0^t du\ \xi(u)\tilde{\mathcal{L}}_I(u)\right]\right\rangle P(X;\, 0) \coloneqq \overleftarrow{\exp}\ [\mathcal{K}(\epsilon,\, t)]P(X;\, 0) \tag{14}$$

with $\mathcal{K}(\epsilon,\, t) = \sum_{i=1}^{\infty} \epsilon^i \mathcal{K}_i(t)$. Keeping up to the second generalized cumulant $\mathcal{K}_2(t) \coloneqq \int_0^t \mathrm{d}u_1 \int_0^{u_1} \mathrm{d}u_2$ $\langle \xi(u_1)\tilde{\mathcal{L}}_I(u_1)\xi(u_2)\tilde{\mathcal{L}}_I(u_2)\rangle$, assuming without loss of generality that $\langle\xi\rangle = 0$, and exploiting (13) we arrive to the following result [52, see the example in section 4.4.2] (note that from the assumption $\langle\xi^2\rangle\tau = 1$ it follows

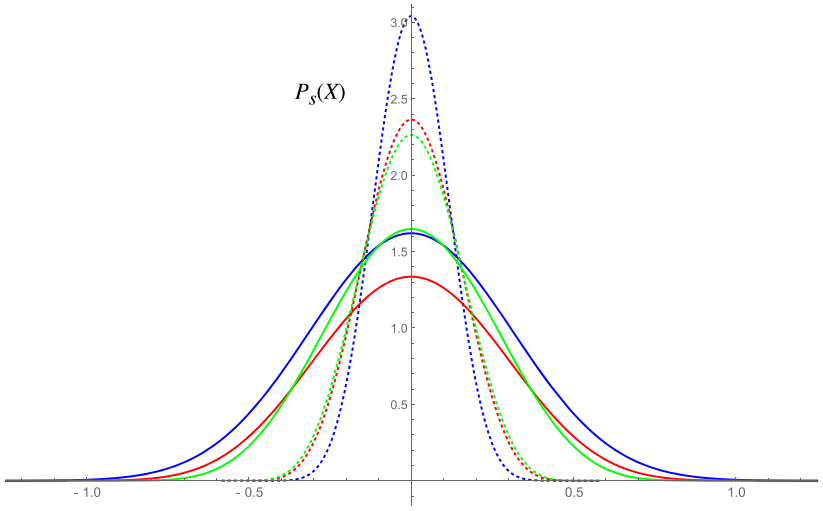


**Figure 1.** The case where $C(X) = \sinh(X)$, and $\langle \xi^2 \rangle = 1$, $\varphi(t) = \exp(-t/\tau)$, $\tau = 0.8$ and $\epsilon = 0.3$. The graphs are the PDFs obtained from (5), in which the state dependent diffusion coefficient $D(X)$ is evaluated from (16) supplemented with the series expansion of (17) truncated at the fifth order. The solid lines refer to even orders: zeroth (blue), second (red) and fourth (green) one. The dashed lines refer to odd orders: first (blue), third (red) and fifth (green) one.

$\langle \xi^2 \rangle = 1/\tau$)

$$\partial_t \tilde{P}(X;\, t) = (\partial_t \mathcal{K}_2(t))\tilde{P}(X;\, t) = \epsilon^2\, \tilde{\mathcal{L}}_I(t) \frac{1}{\tau} \int_0^t du\; \tilde{\mathcal{L}}_I(u) \varphi(t,\, u) \tilde{P}(X;\, t) \tag{15}$$

which coincides with the usual one obtained using a second order in $\epsilon$, Zwanzig projection approach [9, 40, 41, 53, 54].

Getting rid of the interaction picture and exploiting (8) and (11), from (15) we obtain

$$\partial_t P(X;\, t) = \mathcal{L}_a P(X;\, t) + \epsilon^2\, \partial_X \frac{1}{\tau} \int_0^t du\; e^{\mathcal{L}_a^{\times} u}[\partial_X] \varphi(u) P(X;\, t), \tag{16}$$

where $\varphi(u) \coloneqq \varphi(t,\, t-u)$ and, for the sake of simplicity, we have discarded the possible transient regime that would make non stationary the statistics of $\xi(t)$. We stress again that the result (16) is standard in the sense that it can be obtained starting from (6) and using any perturbation approach, where $\epsilon$ is the small parameter (assuming a finite, but not necessarily small, correlation time $\tau$), as the Zwanzig projection method hereafter cited. We have used the generalized cumulant approach, that is based on the identification of the r.h.s. of (13) with a generalized (operator value) characteristic function, because, according to the theory developed in [52], it gives a sound justification of the second order truncation of the full series of generalized cumulants. In other words, the generalized cumulant approach guarantees that the error introduced by using the SDE (15) for the PDF (13) is $O(\epsilon^4 \tau^3)$.

The next step is to rewrite, if possible, (16) as the FPE of (4). To go from (16) to the FPE of (4), the crucial term is the operator $e^{\mathcal{L}_a^{\times} u}[\partial_X]$. In most papers using the Zwanzig projection method (e.g., [39]), the explicit FPE is obtained from (16) assuming that $\tau$, identified with the decay time of the correlation function $\varphi(t)$, is much smaller than the time scale of the unperturbed dynamics driven by the Liouvillian $\mathcal{L}_a$. In this case it is possible to replace, in (16), the power expansion (note the shorthand $(\partial_X C(X)) \coloneqq C'(X)$)

$$e^{\mathcal{L}_a^{\times} u}[\partial_X] = \partial_X + [\mathcal{L}_a,\, \partial_X]\, u + O(u^2) = \partial_X - \partial_X\, C'(X) u + O(u^2). \tag{17}$$

that leads to a FPE with a state dependent diffusion coefficient, given by a series of 'moments' of the time $u$, weighted with the correlation function $\varphi(u)$. However, such a series, as it is apparent from (17), contains secular terms and is (generally) not absolutely convergent. This is clearly shown in the example considered in figure 1. A way to avoid this problem is to solve, without approximations, the Lie evolution of the differential operator $\partial_X$ along the Liouvillian $\mathcal{L}_a$. In [31] this was done for the general case of multidimensional systems and multiplicative forcing. In the present simpler one-dimensional case, recalling that $\mathcal{L}_a = \partial_X C(X)$, the Lie evolution of $\partial_X$, without approximations, can be obtained directly as follows:

$$e^{\mathcal{L}_a^{\times} u}[\partial_X] = e^{\mathcal{L}_a^{\times} u}\left[\partial_X C(X) \frac{1}{C(X)}\right] = e^{\mathcal{L}_a^{\times} u}[\mathcal{L}_a]\, e^{\mathcal{L}_a^{\times} u}\left[\frac{1}{C(X)}\right] = \partial_X C(X) \frac{1}{C(X_0(X;\, -u))} \tag{18}$$

where $X_0(X;\, -u) \coloneqq e^{\mathcal{L}_a^{\times} u}[X] = (e^{-\mathcal{L}_a^{+} u} X)$ is the unperturbed backward evolution, for a time $u$, of the variable of interest, starting from the $X$ position at the initial time $u = 0$. In the last part of (18) we have used two trivial facts (see again [31] for details and generalizations):

- given two operators $\mathcal{A}$ and $\mathcal{B}$, $\mathcal{B}$ does not Lie-evolve along $\mathcal{A}$ when $[\mathcal{A},\ \mathcal{B}] = 0$, thus $e^{\mathcal{L}_a^{\times} u}[\mathcal{L}_a] = \mathcal{L}_a$,
- the Lie evolution along a deterministic (first order partial differential operator) Liouvillian of a regular function $C(X)$, is just the back-time evolution of $C(X)$ along the flow generated by the same Liouvillian:

$$e^{\mathcal{L}_a^{\times} u}[C(X)] = C(X_0(X;\ -u)). \tag{19}$$

Inserting (18) in (16) we get, in a clear and straight way, a generalization of the BFPE of Lopez, West and Lindenberg [38] [4]:

$$\partial_t P(X;\ t) = \mathcal{L}_a P(X;\ t) + \epsilon^2\ \partial_X^2\ \frac{1}{\tau} C(X) \left( \int_0^t du\ \frac{1}{C(X_0(X;\ -u))} \varphi(u) \right) P(X;\ t), \tag{20}$$

namely, the FPE of (4) with the state and time dependent diffusion coefficient

$$D(X,\ t)_{BFPE} = \epsilon^2 \frac{1}{\tau} C(X) \left( \int_0^t du\ \frac{1}{C(X_0(X;\ -u))} \varphi(u) \right) \tag{21}$$

that, for large times, becomes

$$D(X,\ \infty)_{BFPE} = \epsilon^2 \frac{1}{\tau} C(X) \left( \int_0^{\infty} du\ \frac{1}{C(X_0(X;\ -u))} \varphi(u) \right). \tag{22}$$

For weak enough noise intensity $\epsilon$, the BFPE looks like the best possible approximation we can get from a perturbation approach to the SDE of (1). However, this is not the case: the diffusion coefficient in (22) turns out to be wrong, as we are going to show.

It is actually known that in many cases of interest the diffusion coefficient $D(X,\infty)_{BFPE}$, given in (22), becomes negative, giving rise to a non physical negative PDF. A simple example may serve for illustration. Let us consider the case in which $C(X) = \alpha \sinh(kX)$ and $\varphi(t) = \exp(-t/\tau)$, with $\alpha > 0$. The corresponding SDE is related to a well known chemical reaction scheme, see [55]. A straightforward calculation leads to $C(X)/C(X_0(X;\ -u)) = \cosh(\alpha k u) - \cosh(kX)\sinh(\alpha k u)$, which inserted in (22), for times $t \gg \tau/(1 - \alpha k \tau)$, gives ($\theta := \alpha k \tau$)

$$D(X,\ \infty)_{BFPE} = \epsilon^2\ \frac{1 - \theta \cosh(kX)}{1 - \theta}, \tag{23}$$

with the constraint $\theta < 1$. From (23) we see that for $X = \pm \tilde{X}$, with $\tilde{X} := \frac{\ln(\sqrt{\theta^2 - 1} + \theta)}{k}$, the diffusion coefficient of the BFPE vanishes and for $|X| > \tilde{X}$ it is negative which is clearly unphysical. Using (23) in (5), we obtain the stationary PDF:

$$P_s(X)_{BFPE} = \frac{1}{Z_{BFPE}} \left( \frac{1 - \theta \cosh(kX)}{1 - \theta} \right)^{\frac{1 - \theta^2 - k^2 \tau^2 \epsilon^2}{k^2 \tau\ \epsilon^2}} \tag{24}$$

that is affected by the same problem for $|X| > \tilde{X}$. The standard way to cure this flaw of the BFPE is to restrict the support of the PDF [38, 55]. In this case, for example, the first and the second derivatives of (24) vanish in $|X| = \tilde{X}$, therefore one could limit the support of the PDF of (24) to $X \in (-\tilde{X},\ \tilde{X})$. However, from figure 2 it is clear that by increasing $\epsilon$, the result of (24) does not agree well with that obtained from the numerical simulation of the SDE of (1). Only for very small values of $\tau\,\epsilon$ the result is good (i.e, when the width of the PDF is small compared to $2\tilde{X}$). The same problem is present when other drift fields $C(X)$ are considered: the case of $C(X) = X^3$ is shown in appendix, other examples can be found in the literature [42, 56–58].

## 3. The cured BFPE

We show in this section that the flaws of the BFPE are due to an incorrect implementation of the perturbation procedure, and we will cure this situation.

Note first that the possibly negative $D_{BFPE}$ value of (22) is due to the fact that the kernel of the integral can be negative for some $X$ values.

Considering once more the case of $C(X) = \alpha \sinh(kX)$, we see from figure 3, solid lines, that, after a given time $\bar{u}(X)$, the function $C(X)/C(X_0(X;\ -u))$ becomes negative. Note also that the larger the $X$ value, the shorter the time $\bar{u}(X)$. Thus, whatever the correlation decay time $\tau \in (0,\ 1/\alpha k)$, there will always be a certain $\tilde{X}$ value such that $D(X,\ \infty\ )_{BFPE}$ of (22) is negative for $|X| > \tilde{X}$ (the greater the $\tau$ value, the smaller the $\tilde{X}$ value).

[4] Actually, the derivation shown here is a generalization, since we do not assume that $\varphi(t) = \exp(-t/\tau)$ and we do not take the limit $t \to \infty$ in the time integration.

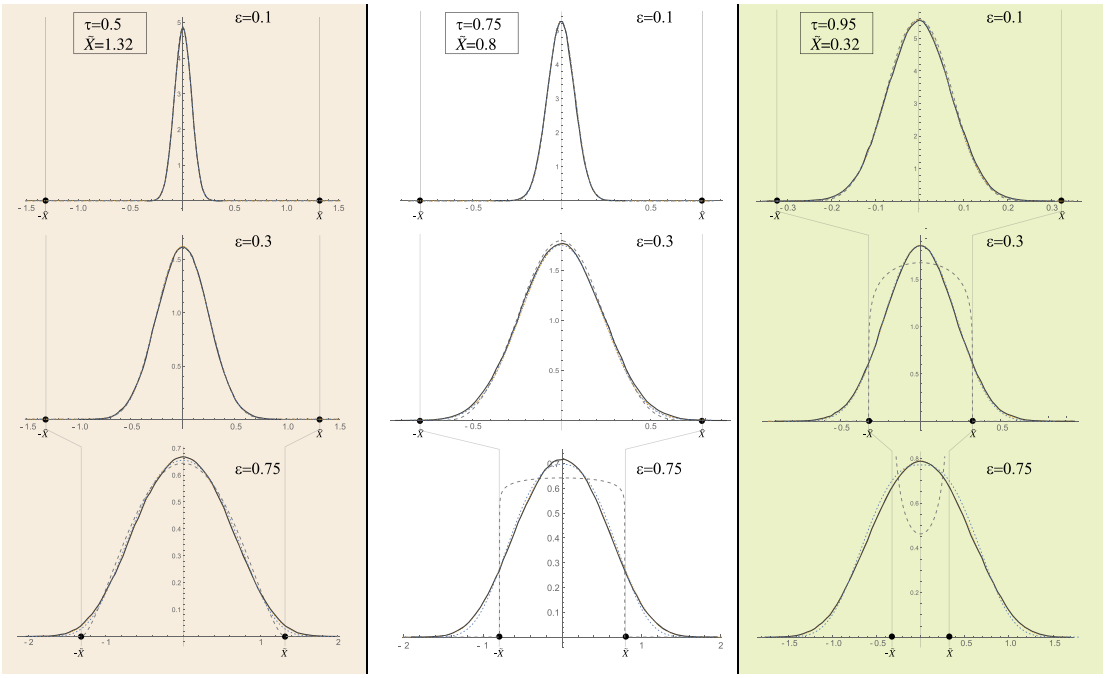


**Figure 2.** Solid black lines: the stationary PDF from the numerical simulation of the SDE of (1) with $C(X) = \alpha \sinh(kX)$ and $\alpha = k = 1$. Dashed gray lines: the BFPE stationary PDF $P_s(X)_{BFPE}$ from (23), the interval $-\tilde{X} < X < \tilde{X}$ is the support of this PDF (see text). Dotted blue lines: the cBFPE stationary PDF $P_s(X)_{cBFPE}$ (discussed further down in this paper) obtained from (5) using $D(X) = D(X, \infty)_{cBFPE}$ of (28). Note how the BFPE PDF completely fails when, increasing $\epsilon$, the width of the PDF becomes comparable (or larger) than the interval width $2\tilde{X}$, whereas there is an excellent agreement between simulations and cBFPE PDF for $\tau$ and $\epsilon$ considered.

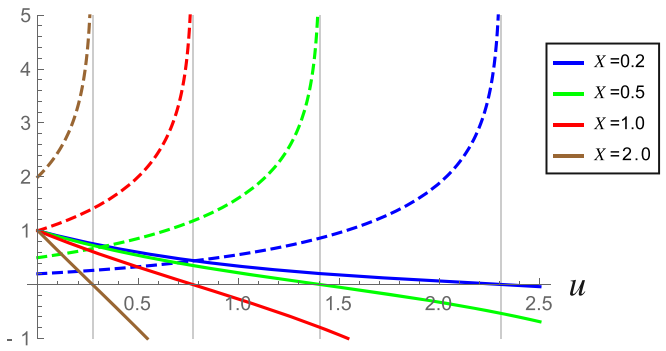


**Figure 3.** Case $C(X) = \sinh(X)$. Solid colored lines: the function $C(X)/C(X_0(X; -u)) = \cosh(u) - \sinh(u)\cosh(X)$ for different initial positions $X_0(X; 0) = X$. Dashed colored lines: the back time evolution $X_0(X; -u) = 2\coth^{-1}\left(e^{-u}\coth\left(\frac{X}{2}\right)\right)$, for the same different initial values $X_0(X; 0) = X$. Thin gray vertical lines: asymptotes at the corresponding time values $\bar{u}(X) = \ln\left(\sqrt{\frac{\cosh(X)+1}{\cosh(X)-1}}\right)$. At the time value $\bar{u}(X)$ where the back time evolution $X_0(X; -u)$ diverges, the function $C(X)/C(X_0(X; -u))$ vanishes. For larger times it is a negative number.

Depending on $C(X)$, we may have rather different scenario: for example, when $C(X) = X^3$ for $|X| > \tilde{X}$, the kernel of the $D(X, \infty)_{BFPE}$ of (22), turns out to be a complex number; see appendix and figure 4. Therefore, in this case it would be seem that the BFPE does not exist at all.

Other interesting examples are the case when $C(X) = -X + \alpha X^3$ (see figure 5), where, depending on the initial $X$, the kernel can go negative ($|X > 1|$) or stay positive ($|X < 1|$); and the case when $C(X) = \alpha \sin(kX)$, where the kernel is always positive (see figure 6).

The shortcomings of the BFPE are however artifacts, introduced by an unappropriate use of the interaction picture, and they can be fixed.

When we go to the interaction picture and then return to the normal representation, we time evolve the variable of interest forth and back, along the flow generated by the $-C(X)$ drift field.

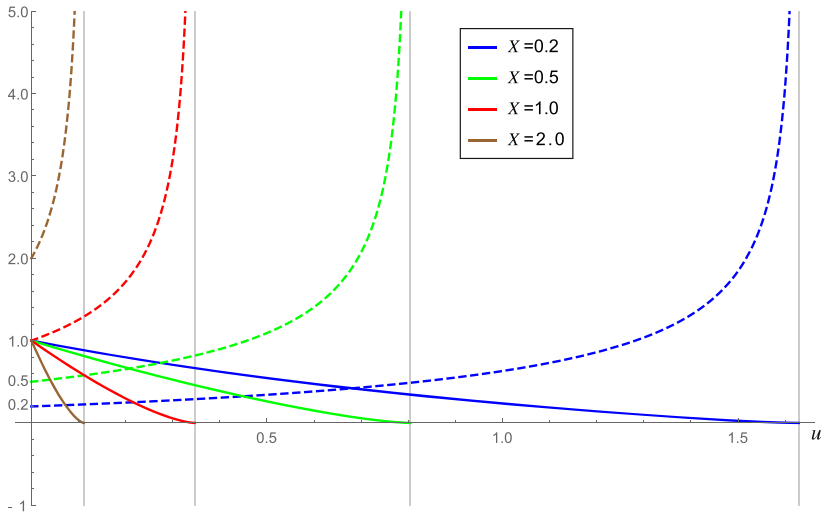


**Figure 4.** Case $C(X) = \alpha X^3$ with $\alpha = 1$. Solid colored lines: the function $C(X)/C(X_0(X; -u)) = e^{u/2}(-2X^2\sinh(u) - \sinh(u) + \cosh(u)^{3/2}$ for different initial positions $X_0(X;0) = X$. Dashed colored lines: the back time evolution $X_0(X; -u) = X/\sqrt{-X^2 + e^{-2u}(1 + X^2)}$, for the same initial values $X_0(X;0) = X$. Thin gray vertical lines: asymptotes at the corresponding time values $\bar{u}(X) = \frac{1}{2}\ln\left(\frac{X^2+1}{X^2}\right)$. At the times $\bar{u}$ when the back time evolution $X_0(X; -u)$ diverges, the function $C(X)/C(X_0(X; -u))$ vanishes, while for larger times it is a complex number.

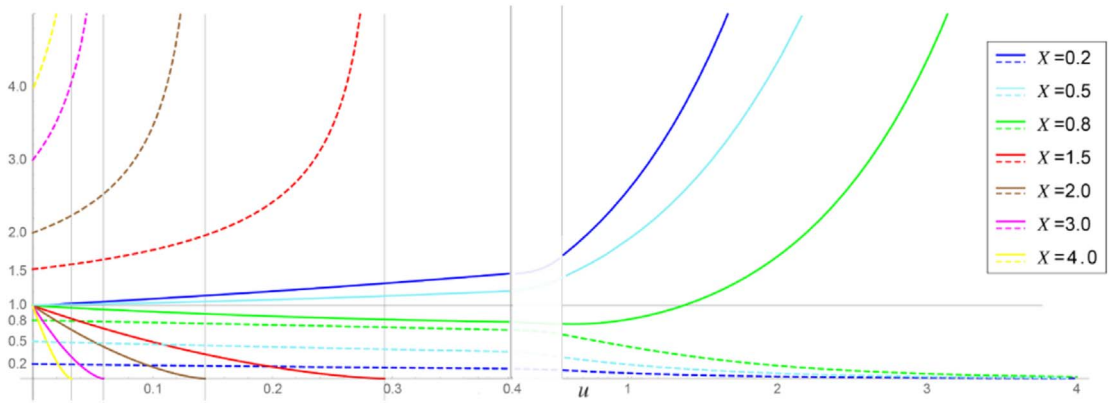


**Figure 5.** Case $C(X) = -X + \alpha X^3, \alpha = 1$. Solid colored lines: $C(X)/C(X_0(X; -u)) = e^u(\sqrt{\alpha(e^{-2u} - 1)X^2 + 1})^3$ for different initial positions $X_0(X;0) = X$. Dashed colored lines: $X_0(X; -u) = e^{-u}X/\sqrt{\alpha(e^{-2u} - 1)X^2 + 1}$ for the same initial values $X_0(X;0) = X$. Thin gray vertical lines: asymptotes at the corresponding time values $\bar{u} = \frac{1}{2}\ln\left(\frac{\alpha X^2}{\alpha X^2 - 1.}\right)$. For $|X| < 1$ the backward trajectories do not diverge at all and the function $C(X)/C(X_0(X; -u)$ is always positive.

The backward evolution is indicated by $X_0 = X_0(X; -u)$. Using (1) we can easily invert this relation, to get $u(X, X_0) = \int_X^{X_0} \frac{1}{C(y)}\, dy$. We define the $X$ dependent time $\bar{u}(X)$ as the time it takes the unperturbed evolution, starting from $X$, to go to $X_0 \to \infty$ , namely

$$\bar{u}(X) \coloneqq u(X, \infty) = \int_X^{\infty} \frac{1}{C(y)}\, dy \tag{25}$$

For a dissipative flow asymptotically limited by a linear function, i.e. with $\lim_{X\to\infty} C(X) \lessapprox X^h$, with $h \leqslant 1$, $u$ is clearly infinite: starting from any position $X$, it takes an infinite time to go backward to $X_0 \to \infty$ . From (25) we see that $\bar{u}(X)$ is infinite also when $C(X)$ has at least one root for some finite value $\tilde{X}$ and $X < \tilde{X}$. However, if in the range $(X, \infty)$ there are no roots of the drift field $C$ and if $\lim_{X\to\infty} C(X) > X^h$, $h > 1$, then we have a finite value for $\bar{u}(X)$: going back in time, the trajectory $X_0(X; -u)$ in a finite time $\bar{u}(X)$ reaches all possible values, greater than $X$. For example, in the case where $C(X) = \alpha\sinh(kX)$ we show in figure 3, dashed lines, that $X_0(X; -u) = \frac{2}{k}\coth^{-1}\left(e^{-\alpha k u}\coth\left(\frac{kX}{2}\right)\right)$ has an asymptote at $u = \bar{u}(X) \coloneqq \frac{1}{k\alpha}\ln\left(\sqrt{\frac{\cosh(kX)+1}{\cosh(kX)-1}}\right)$ (the case $C(X) = X^3$ is shown in figure 4, and the case $C(X) = -X + \alpha X^3$ in figure 5). For 'preceding' times $-u$ with

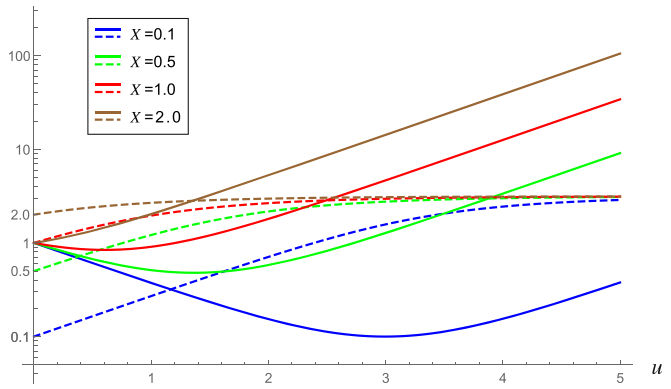


**Figure 6.** Semi-log plot for the case $C(X) = \alpha \sin(kX), \alpha = k = 1$. Solid colored lines: $C(X)/C(X_0(X; -u)) = \cosh(k\alpha u) - \sinh(k\alpha u)\cos(kX)$ for different initial positions $X_0(X; 0) = X$. Dashed colored lines: the back time evolution $X_0(X; -u) = 2\cot^{-1}\left(e^{-k\alpha u}\cot\left(\frac{kX}{2}\right)\right)\Big/k$, for the same initial values $X_0(X; 0) = X$.

$u > \bar{u}(X)$ there are no points in the state-space that are connected to $X$ by the flow generated by the drift field $-C(X)$. This is obviously due to the strong irreversible nature of the flow, that shrinks the state space. In essence, this implies that for such strongly dissipative flows, the backward evolution must be limited to times $u < \bar{u}(X)$, i.e. *we must multiply any function of* $X_0(X; -u)$ *by the Heaviside function* $\Theta(\bar{u}(X) - u)$. Therefore, the BFPE state dependent diffusion coefficient of equations (21)–(22) must be corrected as follows (cBFPE stands for corrected BFPE):

$$D(X, t)_{cBFPE} = \epsilon^2 \frac{1}{\tau} C(X)\left(\int_0^t du \, \frac{\Theta(\bar{u}(X) - u)}{C(X_0(X; -u))}\varphi(u)\right) \tag{26}$$

$$D(X, \infty)_{cBFPE} = \epsilon^2 \frac{1}{\tau} C(X)\left(\int_0^{\bar{u}(X)} du \, \frac{1}{C(X_0(X; -u))}\varphi(u)\right) = D(X, \bar{u}(X))_{BFPE} \tag{27}$$

*equations (26)–(27) are the main result of the present work*. Concerning the stationary PDF, the correct result is obtained using (27) in (5).

For the case $C(X) = \alpha \sinh(kX)$, from (27) we get:

$$D(X, \infty)_{cBFPE} = \frac{\epsilon^2\left(\alpha k\tau(\cosh(kX) + 1)\left|\tanh\left(\frac{kX}{2}\right)\right|^{\frac{\alpha k\tau+1}{\alpha k\tau}} - \tau\cosh(kX) + 1\right)}{1 - (\alpha k\tau)^2}. \tag{28}$$

The state dependent diffusion coefficient $D(X, \infty)_{cBFPE}$ of (28) is always positive. The stationary PDF for this case is obtained using (28) in (5). Because of the integral in the exponent in (5), an analytical expression cannot be obtained: the results of numerical integration, for different values of $\tau$ and $\epsilon$, are shown in figure 2. We can see that the stationary PDFs of the corrected BFPE are quite close to those obtained from the numerical integration of the SDE, even for large $\tau$ values and relatively large $\epsilon$. In the case of $C(X) = X^3$, $D(X, \infty)_{cBFPE}$ of (27) and the corresponding stationary PDF are now real quantities, see appendix and figures A1 and A2.

We would like to add a few comments about the divergence of the backward evolution $X_0(X; -u)$: we have seen that there are drift fields $C(X)$ such that for any initial position $X_0(X; 0) = X$, the backward evolution diverges with an asymptote at a given finite time $\bar{u}(X) = \int_X^\infty \frac{1}{C(y)}\, dy$. This behaviour is shown in figures 3 and 4. These are cases where $C(X)$ has not roots and $\lim_{X\to\infty} C(X) > X^h$ with $h > 1$. However, when $C(X)$ has $n \in N$ roots at $\tilde{X}_1 < \tilde{X}_2 < \ldots < \tilde{X}_n$, then the possible divergence of the backward evolution depends on $X$. In fact, for $X < \tilde{X}_i$, $1 \leqslant i \leqslant n$ we have $u(X, X_i) = \int_X^{X_i} \frac{1}{C(y)}\, dy = \infty$, from which (see the definition (25)) $\bar{u}(X) = \infty$, while for $X > X_n$ the divergence of the backward evolution depends on the asymptotic behavior $(X \to \infty)$ of $C(X)$. In other words, the possible correction of the BFPE can depend on the variable of interest $X$. A case of this type is shown in figure 5.

On the other hand, the important case of Brownian motion in a periodic potential, a heuristic model with applications in various branches of science and technology, like the diffusive dynamics of atoms and molecules on crystal surfaces [59], modelled using $C(X) = \alpha \sin(kX)$, is such that $\bar{u}(X) = \infty \; \forall X$. In fact, the function $C(X)/C(X_0(X; -u))$ is always positive and simply increases with $u$ as $e^{k\alpha u}$. Therefore in this case the 'standard' BFPE formula of (21) for the diffusion coefficient is correct.

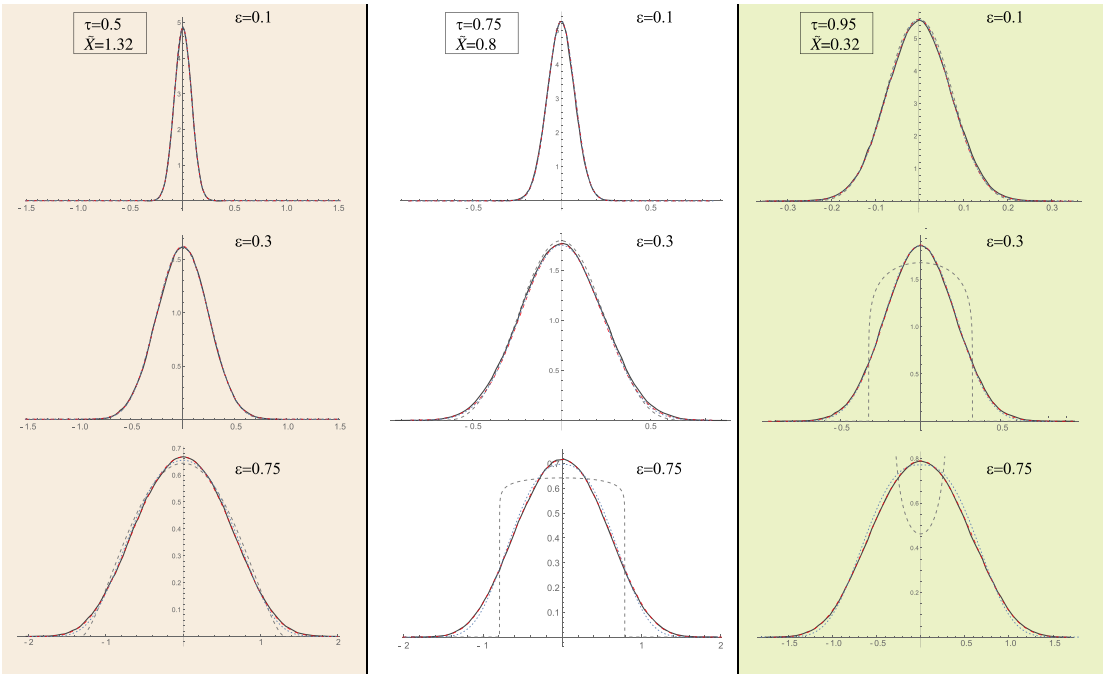


**Figure 7.** The same as figure 2 but without the $P_s(X)_{BFPE}$ and with inserted the $P_s(X)_{LLA}$. Solid black lines: the stationary PDF from the numerical simulations of the SDE of (1) with $C(X) = \sinh(X)$. Dotted blue lines: the cBFPE stationary PDF $P_s(X)_{cBFPE}$ obtained from (5) using $D(X) = D(X, \infty)_{cBFPE}$ of (28). Dashed red lines (barely visible close or under the solid lines): $P_s(X)_{LLA}$ of (34). The three columns correspond to three different values for $\tau$, while the three rows corresponds to three different values for $\epsilon$. Note the excellent agreement between simulations and LLA PDF.

## 4. A comparison with the Local Linearization Approach

As we mentioned in the Introduction, very often the LLA FPE turns out to be fairly close to the numerical simulations. This is shown in figure 7, for the case $C(X) = \alpha \sinh(kX)$. We are going to show that this is not a coincidence: as a matter of fact, the LLA FPE is an excellent approximation of the cBFPE, when the latter is applicable (i.e., typically, small $\epsilon$ and finite, but not small, $\tau$).

We need to briefly go through the derivation of the LLA FPE. West *et al* have shown [38] that the LLA FPE can be formally derived from the BFPE of (20) as follows:

a. there is a large enough time-scale separation between the unperturbed dynamics and the decay time of the correlation function $\varphi(t)$, so that the unperturbed dynamics $X_0(X; -u)$ can be considered close to the initial position $X$;

b. given the point "a" above, rather than expanding $\frac{1}{C(X_0(X;-u))}$ in powers of $u$ (which would give rise to the same secular terms as the expansion in (17)), expand its logarithm

$$\frac{1}{C(X_0(X;-u))} = \exp\left[\ln\left(\frac{1}{C(X_0(X;-u))}\right)\right] = \exp\left[\ln\left(\frac{1}{C(X)}\right) - C'(X)u - \frac{1}{2}C(X)C''(X)u^2 + O(u^3)\right] \tag{29}$$

and truncate the series at the first order.

Using point b in (20), we are led to the LLA FPE (here generalized to finite times and to a generic correlation function of the noise):

$$\partial_t P(X;\, t) \sim \mathcal{L}_a P(X;\, t) + \epsilon^2 \frac{1}{\tau} \partial_X^2 \left( \int_0^t du\; e^{-C'(X)u} \varphi(u) \right) P(X;\, t). \tag{30}$$

Note that for $C(X) = \gamma X$, the series expansion of the r.h.s. of (29) stops *exactly* at the first order in $u$, while this does not happen expanding the term $1/C(X_0(X; -u))$. Therefore, instead of using the West *et al* approach (given by a–b above) to go from the BFPE to the LLA FPE, the latter can be directly obtained by replacing the function $C(X)/C(X_0(X; -u))$ with an exponential function with state dependent decay coefficient $C'(X)$: $C(X)/C(X_0(X; -u)) \to \exp(-C'(X)u)$. From (30) we get the following result for the state dependent

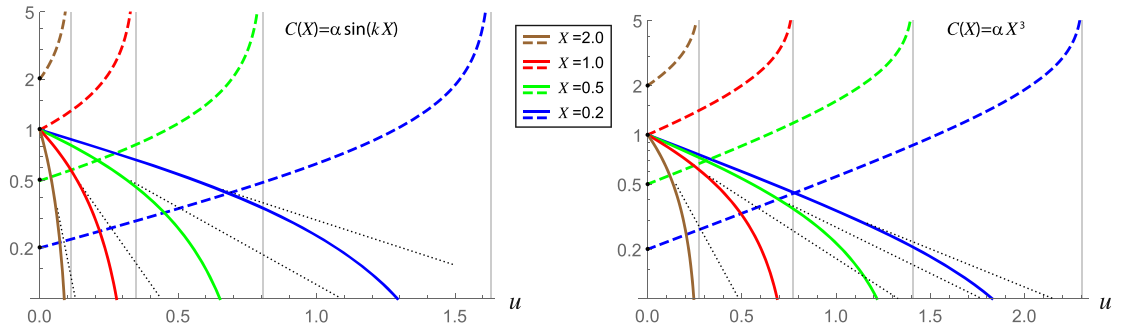


**Figure 8.** Left (right), the same of figure 3 (figure 4) but in log scale. The dotted black lines correspond to the LLA approximation. We can see that the deviation from the exponential decay of the function $C(X)/C(X_0(X;-u))$ (solid lines) is relevant only in the final part, where the value of the function is relatively small.

diffusion coefficient of the FPE:

$$D(X,\,t)_{LLA} = \epsilon^2 \frac{1}{\tau}\left(\int_0^t du\; e^{-C'(X)u}\varphi(u)\right) \tag{31}$$

that, for large times becomes

$$D(X,\,\infty)_{LLA} = \epsilon^2\,\frac{\hat{\varphi}(C'(X))}{\tau} \tag{32}$$

where $\hat{\varphi}$ stands for Laplace transform of $\varphi$. From (32) it turns out that $D(X,\,\infty)_{LLA}$ exists and is positive under fairly general conditions. For example, considering again the case $C(X) = \alpha\,\sinh(kX)$, from (32) we easily get

$$D(X,\,\infty)_{LLA} = \frac{\epsilon^2}{1 + \alpha k\tau\,\cosh(kX)}, \tag{33}$$

where the only constraint is that the flow is not divergent (i.e. $\alpha > 0$). Using (33) in (5) we obtain the LLA stationary PDF for this case:

$$P_s(X)_{LLA} = \frac{1}{Z_{LLA}}\left(\frac{1 + \alpha k\tau\,\cosh(kX)}{1 + \alpha k\tau}\right) \times \exp\left(-\frac{\alpha\,\sinh^2\left(\frac{kX}{2}\right)(\alpha k\tau + \alpha k\tau\,\cosh(kX) + 2)}{k\epsilon^2}\right) \tag{34}$$

In appendix we report the LLA results for the cubic case. In figure 7 we can see the stationary PDFs of the LLA FPE, together with the results from the cBFPE: the agreement with the numerical integration of the SDE of (1) is very good.

Figure 8 compares the kernels of the cBFPE and of the LLA for the cases $C(X) = \alpha\,\sinh(kX)$ and $C(X) = \alpha X^3$. It turns out that the LLA kernel (dotted lines) is an excellent approximation of the cBFPE kernel. It is hence not surprising that the LLA PDF is as close to the simulations as it is the cBFPE PDF.

This is a nice explanation of what has been down heuristically in the literature: the LLA approach of Grigolini [42, 60] is indeed based on the assumption that, for any value of $X$, we can safely replace the unperturbed *backward* evolution of the function $f(X,\,u) \coloneqq C(X)/C(X_0(X;-u))$, with an exponential function of the time $u$, with the $X$ dependent exponent: $f(X,\,u) \sim \exp[-C'(X)u]$. For one-dimensional dissipative systems, the exponential behavior of such a *back* time evolution is typical.

Actually, there is another general argument, not related to the cBFPE, that leads us to speculate that typically (but not always), the LLA FPE works well, also for strong perturbations. In fact it is possible to prove that the LLA and the Fox functional-calculus [33, 34] corresponds to the Almost Gaussian Assumption for generalized stochastic operators [52]: independently of the value of $\epsilon$, *when* $\xi(t)$ is a Gaussian stochastic process, the LLA typically makes almost vanishing *all* the terms, appearing in the projection/cumulant expansion, which would destroy the FPE. This means that *often* the LLA FPE would be valid even for large $\epsilon$ values for which the cBFPE breaks down.

On the other hand, if the stochastic process $\xi(t)$ is not Gaussian, or it is not at all stochastic (for example, it is the degree of freedom of a chaotic dynamical system), then the Almost Gaussian Assumption or the Fox functional calculus can no longer be advocated to give an *a priori* justification (although weak) to the LLA FPE. In these cases, a small $\epsilon$ value and the cBFPE would be the only possible approach for a proper FPE treatment, and the LLA FPE could be, at the best, an approximation of the cBFPE.

## 5. Conclusions

By definition, the BFPE is the best FPE we can get from a perturbation approach starting from a SDE. In this work we are interested in the 1-d case with additive noise as in (1), in which $\epsilon$ is the small parameter. For the 1-d case the BFPE was obtained many years ago by Lopez, West and Lindenberg [38], but their result reveals unphysical features. In particular, if $\tau$ and $\epsilon$ are not fairly small, it may lead to negative values both of the diffusion coefficient and of the PDF, in some region of the state space. It is customary to cure this situation by simply restricting the domain of support of the PDF to exclude these regions. It has been argued that this unphysical result of the BFPE might point to problems in the model used to represent the physical system [61]. In this work we show, on the contrary, that these problems are due to an incorrect use of the perturbation approach for dissipative systems. In particular, a proper use of the interaction picture fixes the problem. The cBFPE gives results that are close to those of numerical simulations of the SDE of (1), even for values of $\epsilon$ and $\tau$ well beyond those allowed by the classical BFPE. The stationary PDF is now similar also to that obtained from the LLA FPE of Grigolini [42, 60] and Fox [34].

## Appendix. The cubic case

We briefly present the results for the pure cubic case $C(X) = X^3$. This is an extreme non linear case because even small oscillations are non-linear. It is no coincidence that the standard BFPE cannot be used in this case (see below).

From (21) we obtain

$$D(X,\,t)_{BFPE} = \epsilon^2\,\frac{1}{2}\,e^{-\frac{t}{\tau}}\Bigg[(2\sqrt{1-2tX^2}\,e^{\frac{1}{2\tau X^2}}(2tX^2+3\tau X^2-1) - 3\sqrt{2\pi}\,\tau^{3/2}X^3e^{t/\tau}\,\mathrm{erfi}\left(\frac{\sqrt{\frac{1}{2}-tX^2}}{\sqrt{\tau}X}\right)\Bigg]e^{-\frac{1}{2\tau X^2}} - \frac{1}{2}\tau\left[-3\sqrt{2\pi}\,\tau^{3/2}X^3e^{-\frac{1}{2\tau X^2}}\,\mathrm{erfi}\left(\frac{1}{\sqrt{2}\,\sqrt{\tau}X}\right)+6\tau X^2-2\right] \tag{A.1}$$

that, for $t > 2X^2$ *is a complex number*: for large times it is not defined. This means that for a cubic drift field, by using the standard BFPE a stationary PDF cannot be obtained. The situation is different exploiting our correction to the BFPE. In fact, for large times ($t \to \infty$), we have (see (27)

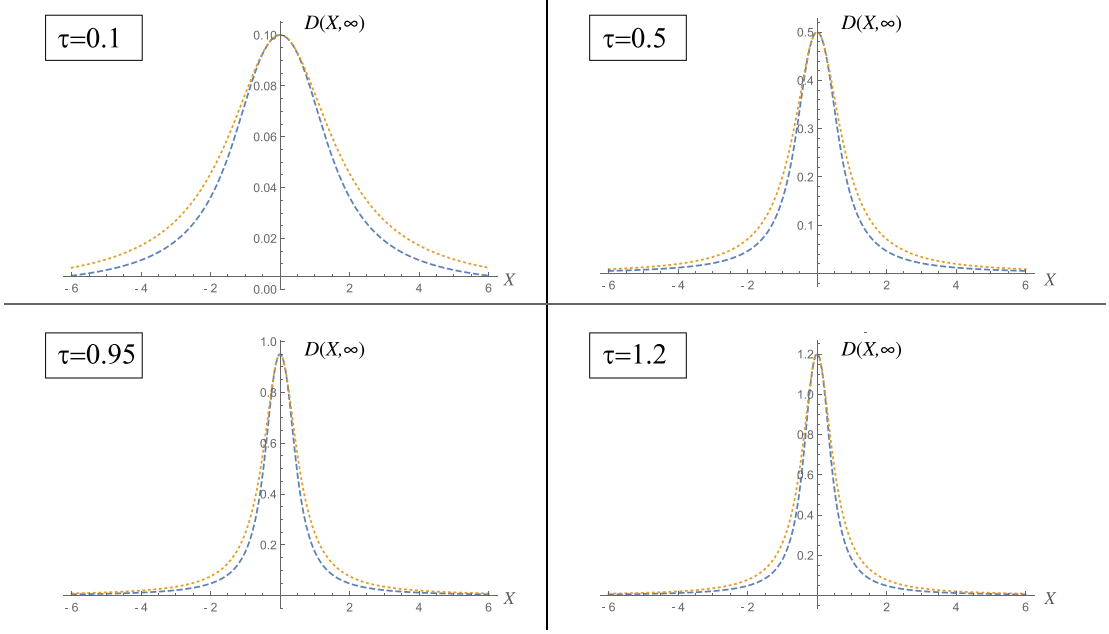


**Figure A1.** Diffusion coefficients for a pure cubic drift field. The BFPE gives an imaginary result, thus in this case cannot be used. Dashed blue lines: the $D(X,\,\infty)_{cBFPE}$ of (A.2) for different values of $\tau$. Dotted orange line: the $D(X,\,\infty)_{LLA}$ of (A.3) for the same values of $\tau$.

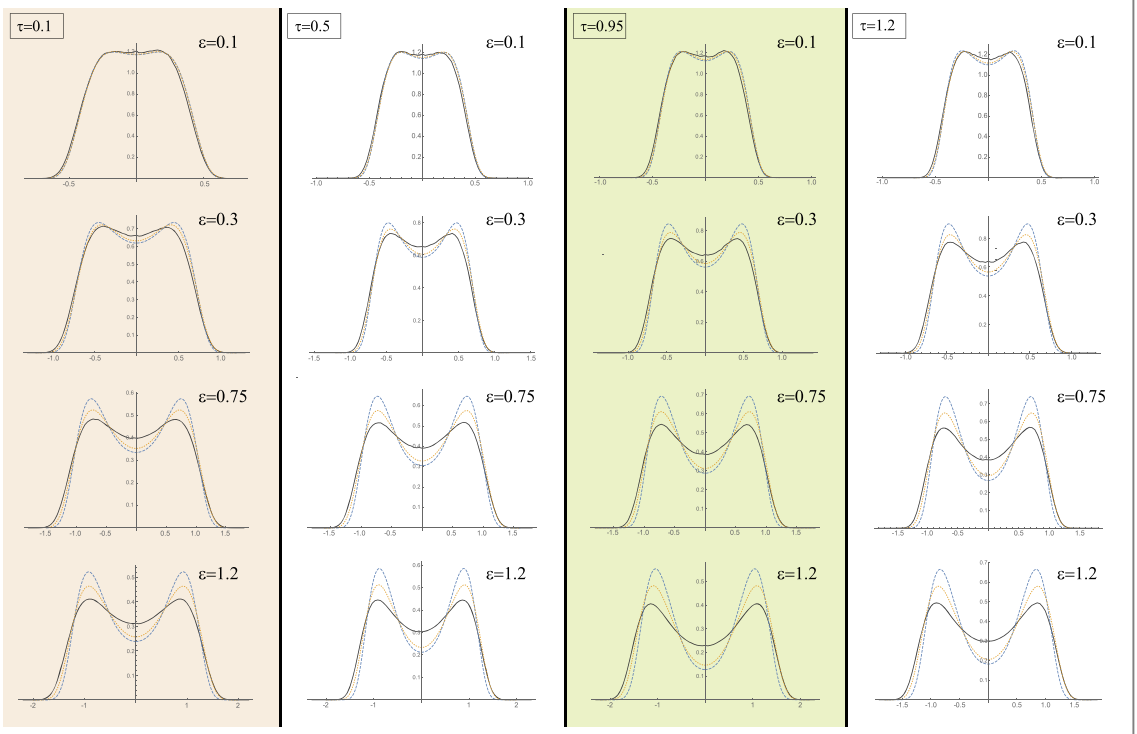


**Figure A2.** The stationary PDF for the SDE of (1) where $C(X) = X^3$ and $\xi(t)$ is a Gaussian noise with correlation function $\varphi(t) = \exp(-t/\tau)$. In this case the standard BFPE *cannot* be used because it leads to an imaginary diffusion coefficient $D(X, \infty)_{BFPE}$ (see text). The four columns correspond to four different values for $\tau$, while the four rows corresponds to four different values for $\epsilon$. Solid black lines: the results of the numerical simulation of the SDE. Dashed blue lines: the cBFPE results, the PDF of (5) where the diffusion coefficient is given in (A.2). Dotted orange lines: the LLA result, the PDF of (5) where the diffusion coefficient is given in (A.3).

$$D(X, \infty)_{cBFPE} = D(X, \bar{u}(X))_{BFPE} = \epsilon^2\left[1 + 3\tau X^2\left(\sqrt{2}\sqrt{\tau}XF\left(\frac{1}{\sqrt{2}X\sqrt{\tau}}\right) - 1\right)\right] \tag{A.2}$$

where $F(x) := e^{-x^2}\int_0^x e^{y^2}\,dy = e^{-x^2}\frac{\sqrt{\pi}}{2}\mathrm{erfi}(x)$ is the Dawson function. The diffusion coefficient of (A.2) is now positive and well defined for any $X$. Concerning the LLA diffusion coefficient, from (32) we easily get:

$$D(X, \infty)_{LLA} = \frac{\epsilon^2}{3\tau X^2 + 1}. \tag{A.3}$$

In figure A1 we compare the corrected BFPE and the LLA diffusion coefficients, respectively. Inserting in (5) the expressions in equations (A.2))–(A.3)), we obtain the stationary PDF shown in figure A2. We see that in this extreme non linear case, where the standard BFPE cannot be used, our corrected BFPE gives results that, for small $\epsilon$, are in agreement with numerical simulations of the SDE. Notice that, in this case, also the LLA fails for large $\epsilon$ values.

## ORCID iDs

Marco Bianucci https://orcid.org/0000-0002-0276-2813
Riccardo Mannella https://orcid.org/0000-0002-0049-2506

## References

[1] Schadschneider A, Chowdhury D and Nishinari K (ed) 2010 *Stochastic Transport in Complex Systems. From Molecules to Vehicles* (Amsterdam: Elsevier) (http://sciencedirect.com/science/book/9780444529657) (https://doi.org/10.1080/00107514.2011.647088)
[2] Zhu S, Yu A W and Roy R 1986 *Phys. Rev.* A **34** 4333–47
[3] Zhu S 1993 *Phys. Rev.* A **47** 2405–8
[4] Da-jin W, Li C and Bo Y 1989 *Commun. Theor. Phys.* **11** 379
[5] Dong-Cheng M, Guang-Zhong X, Li C and Da-jin W 1999 *Acta Phys. Sin., Overseas Ed.* **8** 174
[6] Zhu P and Zhu Y J 2010 *Int. J. Mod. Phys.* B **24** 2175–88
[7] Oliveira F 1998 *Physica A* **257** 128–35
[8] Fonseca T, Grigolini P and Pareo D 1985 *J. Chem. Phys.* **83** 1039–48
[9] Bianucci M and Grigolini P 1992 *J. Chem. Phys.* **96** 6138–48

[10] Bianucci M, Grigolini P and Palleschi V 1990 *J. Chem. Phys.* **92** 3427–41
[11] Lebreuilly J, Wouters M and Carusotto I 2016 *C.R. Phys.* **17** 836–60 polariton physics / Physique des polaritons
[12] Horsthemke W and Lefever R 1984 *Noise-Induced Transitions. Theory and Applications in Physics, Chemistry, and Biology* (*Springer Series in Synergetics, 1st edn* vol 15) (Berlin Heidelberg: Springer) (http://springer.com/gp/book/9783540113591?wt_mc=ThirdParty.SpringerLink.3.EPR653.About_eBook#otherversion=9783540368526) (https://doi.org/10.1007/3-540-36852-3)
[13] Zhang H, Yang T, Xu W and Xu Y 2014 *Nonlinear Dyn.* **76** 649–56
[14] Jin F F, Lin L, Timmermann A and Zhao J 2007 *Geophys. Res. Lett.* **34** L03807
[15] Bianucci M 2016 *Geophys. Res. Lett.* **43** 386–94
[16] Harne R L and Wang K W 2013 *J. Vib. Acoust.* **136** 021009.1-021009.8 (*Preprint* https://asmedigitalcollection.asme.org/vibrationacoustics/article-pdf/136/2/021009/6340583/vib_136_02_021009.pdf)
[17] Daqaq M F 2011 *J. Sound Vib.* **330** 2554–64
[18] Spanio T, Hidalgo J and Muñoz M A 2017 *Phys. Rev.* E **96** 042301
[19] Ridolfi L, D'Odorico P and Laio F 2011 *Noise-Induced Phenomena in the Environmental Sciences* (Cambridge: Cambridge University Press) (https://doi.org/10.1017/CBO9780511984730)
[20] Zeng C, Xie Q, Wang T, Zhang C, Dong X, Guan L, Li K and Duan W 2017 *Ecosphere* **8** e01805
[21] Venturi D, Sapsis T P, Cho H and Karniadakis G E 2012 *Proc. of the Royal Society A: Mathematical, Physical and Engineering Sciences* **468** 759–83
[22] Zeng C and Wang H 2010 *J. Stat. Phys.* **141** 889–908
[23] Yang T, Han Q L, Zeng C H, Wang H, Liu Z Q, Zhang C and Tian D 2014 *Indian J. Phys.* **88** 1211–9
[24] Li S H and Zhu Q X 2018 *Chin. J. Phys.* **56** 346–54
[25] Li X L and Ning L J 2016 *Indian J. Phys.* **90** 91–8
[26] Bose T and Trimper S 2012 *Physica Status Solidi (b)* **249** 172–80
[27] Chattopadhyay A K and Aifantis E C 2016 *Phys. Rev.* E **94** 022139
[28] Adelman S A 1976 *J. Chem. Phys.* **64** 124–30
[29] Kubo R 1962 *J. Phys. Soc. Jpn.* **17** 1100–20
[30] Kubo R 1963 *J. Math. Phys.* **4** 174–83
[31] Bianucci M 2018 *J. Math. Phys.* **59** 053303
[32] Mamis K I, Athanassoulis G A and Kapelonis Z G 2019 *Proc. of the Royal Society A: Mathematical, Physical and Engineering Sciences* **475** 20180837
[33] Fox R F 1986 *Phys. Rev.* A **33** 467–76
[34] Fox R F 1986 *Phys. Rev.* A **34** 4525–7
[35] Hänggi P 1989 Colored noise in continuous dynamical systems: a functional calculus approach *Noise in Nonlinear Dynamical Systems: Theory of continuous Fokker-Planck systems* ed F Moss and P V E McClintock (Cambridge: Cambridge University Press) pp 307–28
[36] Hänggi P and Jung P 1994 Colored noise in dynamical systems *Noise in Nonlinear Dynamical Systems: Theory of continuous Fokker-Planck systems* (*Adv. Chem. Phys.* vol 89) ed I Prigogine and S A Rice (New York: An Interscience Publication, Wiley) Ch 4 239–326
[37] Hänggi P, Mroczkowski T J, Moss F and McClintock P V E 1985 *Phys. Rev.* A **32** 695–8
[38] Peacock-López E, West B J and Lindenberg K 1988 *Phys. Rev.* A **37** 3530–5
[39] Grigolini P and Marchesoni F 1985 Basic description of the rules leading to the adiabatic elimination of fast variables *Memory Function Approaches to Stochastich Problems in Condensed Matter* (*Adv. Chem. Phys.* vol LXII) ed M W Evans, P Grigolini and G P Parravicini (New York: An Interscience Publication, Wiley) ch 2, p 556
[40] Grigolini P 1989 The projection approach to the Fokker-Planck equation: applications to phenomenological stochastic equations with colored noises *Theory of Continuous Fokker-Planck Systems* (*Noise in Nonlinear Dynamical Systems* vol 1) (Ed.),) ed F Moss and P V E McClintock (Cambridge, England: Cambridge University Press) ch 5, p 161 (http://ebooks.cambridge.org/ebook.jsf?bid=CBO9780511897818) 9780511897818 (https://doi.org/10.1017/CBO9780511897818)
[41] Bianucci M 2015 *J. Stat. Mech: Theory Exp.* **2015** P05016
[42] Tsironis G P and Grigolini P 1988 *Phys. Rev.* A **38** 3749–57
[43] Colet P, Wio H S and San Miguel M 1989 *Phys. Rev.* A **39** 6094–7
[44] Sancho J M, Miguel M S, Katz S L and Gunton J D 1982 *Phys. Rev.* A **26** 1589–609
[45] Sancho J M and San Miguel M 1980 *Zeitschrift f' ×ur Physik B Condensed Matter* **36** 357–64
[46] Sancho J M S M M 1989 Langevin equations with colored noise *Theory of Continuous Fokker-Planck Systems* (*Noise in Nonlinear Dynamical Systems) (Ed.),*) ed F Moss and P V E McClintock vol 1 (Cambridge: Cambridge University Press) 72–109 ch 3
[47] Jung P and Hänggi P 1987 *Phys. Rev.* A **35** 4464–6
[48] Duan W L and Fang H 2020 *Physica A* **555** 124624
[49] Mamis K, Athanassoulis G and Papadopoulos K 2018 *Procedia Computer Science* **136** 164–73 VII International Young Scientists Conf. on Computational Science, YSC2018, 02-06 July 2018, Heraklion, Greece
[50] Athanassoulis G A and Mamis K I 2019 *Phys. Scr.* **94** 115217
[51] Gardiner C 2009 *Stochastic Methods. A Handbook for the Natural and Social Sciences IV ed (Springer Series in Synergetics vol 13)* (Berlin Heidelberg: Springer) (http://springer.com/gp/book/9783540707127#reviews)
[52] Bianucci M and Bologna M 2020 *J. Stat. Mech: Theory Exp.* **2020** 043405
[53] Zwanzig R (ed) 2001 *Nonequilibrium Statistical Mechanics* (Oxford: Oxford University Press) (http://ukcatalogue.oup.com/product/9780195140187.do)
[54] Bianucci M, Mannella R, West B J and Grigolini P 1995 *Phys. Rev.* E **51** 3002–22
[55] Lindenberg K and West B J 1983 *Physica A* **119** 485–503
[56] Masoliver J, West B J and Lindenberg K 1987 *Phys. Rev.* A **35** 3086–94
[57] Tsironis G P and Grigolini P 1988 *Phys. Rev. Lett.* **61** 7–10
[58] Grigolini P, Lugiato L A, Mannella R, McClintock P V E, Merri M and Pernigo M 1988 *Phys. Rev.* A **38** 1966–78
[59] Ala-Nissila T, Ferrando R and Ying S C 2002 *Adv. Phys.* **51** 949–1078
[60] Faetti S, Fronzoni L, Grigolini P and Mannella R 1988 *J. Stat. Phys.* **52** 951–78
[61] Peacock-López E, de la Rubia F J, West B J and Lindenberg K 1989 *Phys. Lett.* A **136** 96–102